Supplemental Appendix

Right heart failure in mice upon pressure overload is promoted by mitochondrial oxidative stress

Table of contents

1. Supplemental Figures and Legends 2
Figure S1. 2
Figure S2. 3
Figure S3. 3
Figure S4. 4
Figure S5. 5
Figure S6. 6
Figure S7. 7
Figure S8. 8
Figure S9. 8
Figure S10. 9
2. Supplemental Methods 10
Animal Experimental Protocols 10
Immunohistochemistry and Immunofluorescence 10
Quantitative Real Time PCR 11
3. Supplemental References 12

1. Supplemental Figures and Legends

Figure S1

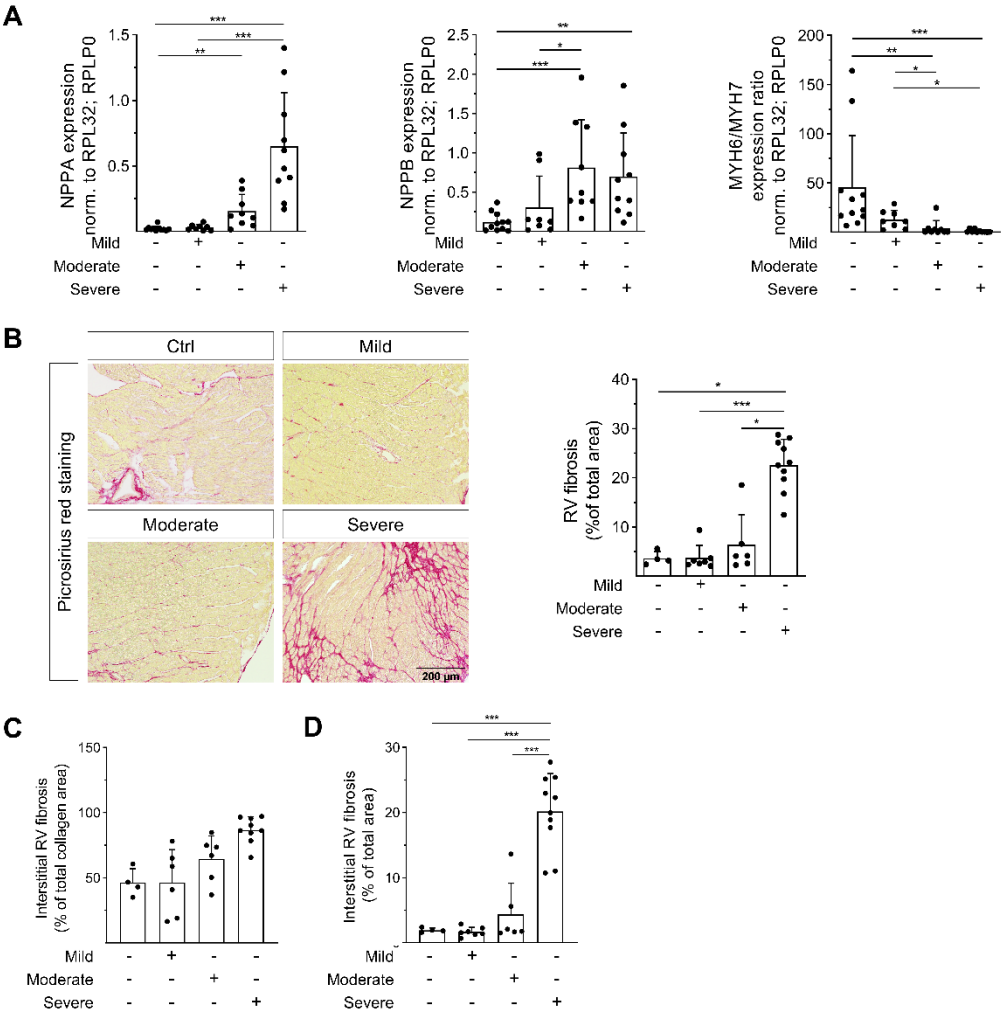

Figure S1. Right ventricular remodeling in 6J mice upon pulmonary artery banding. A) mRNA expression of atrial natriuretic peptide (NPPA) and brain natriuretic peptide (NPPB), as well as the relation of alpha-myosin heavy chain (MYH6) to beta-myosin heavy chain (MYH7) expression were altered with increasing stenosis degree of PAB (N=11/8/9/10 mice). B) Representative images of picrosirius red stained sections (scale bar=200µm) and morphometric analysis of the fibrotic area (interstitial plus perivascular) showing increasing fibrosis with degree of PAB (N=4/7/6/10 mice). C) Percentage of interstitial fibrosis related to total fibrotic area (interstitial plus perivascular) slightly increased with increasing stenosis grade (N=4/7/6/10 mice). D) Percentage of interstitial fibrotic area related to total tissue section area, increased with increasing stenosis grade (N=4/7/6/10 mice). Statistical significance was calculated with Kruskal-Wallis test followed by Dunn's multiple comparison test. *p < 0.05; **p < 0.01; ***p < 0.001.

Figure S2

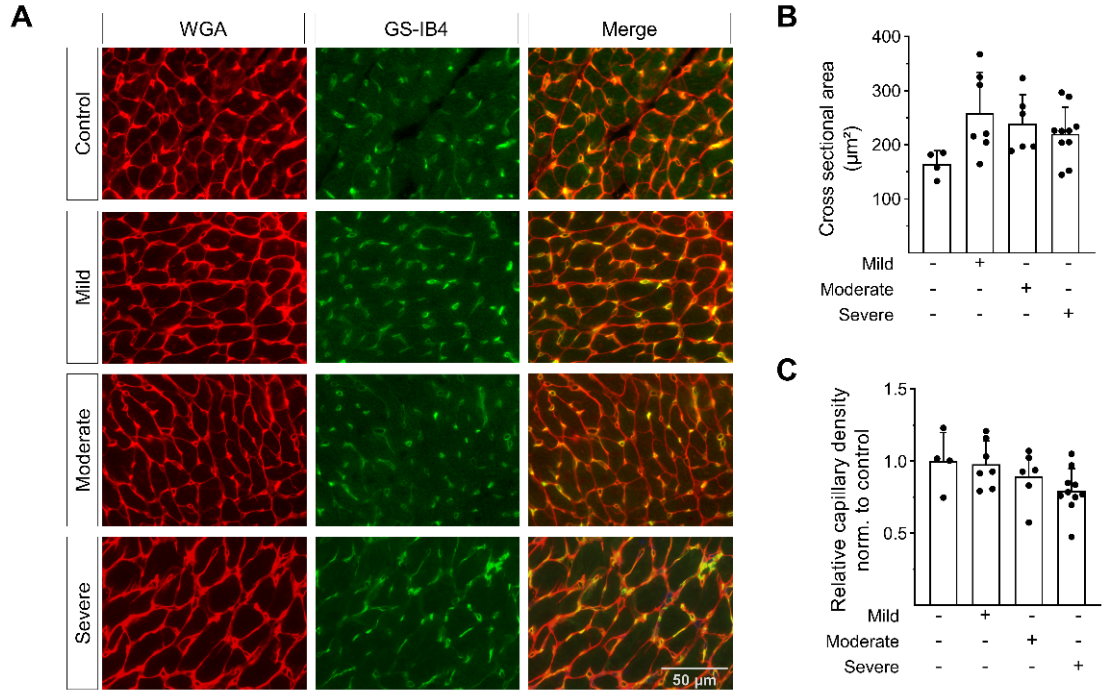

Figure S2. Right ventricular cardiomyocyte cross-sectional area and capillary density in 6J mice upon pulmonary artery banding. A) Representative images of staining for cardiomyocyte cross-sectional area analysis using wheat germ agglutinin (WGA) and capillary density using isolectin of griffonia simplicifolia (GSI-B4). Scale bar=50µm. B) Cross-sectional area of RV cardiomyocytes was enhanced after mild, moderate and severe PAB (N=4/7/6/10 mice). C) Capillary density was slightly and progressively diminished after 2 weeks of moderate and severe PAB (N=4/7/6/10 mice). It was tested for statistical significance with Kruskal-Wallis test followed by Dunn's multiple comparison test.

Figure S3

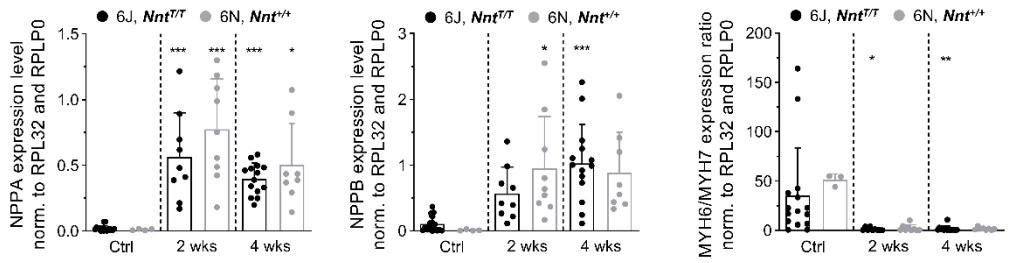

Figure S3. Expression of fetal gene program markers after pulmonary artery banding. mRNA expression of atrial natriuretic peptide (NPPA), brain natriuretic peptide (NPPB) (N=16/4/9/9/14/8 mice) and the relation of alpha-myosin heavy chain (MYH6) to beta-myosin heavy chain (MYH7) (N=15/3/9/9/14/8 mice) was not significantly altered between 6J and 6N mice after 2 and 4 weeks of

PAB. Statistical significance was calculated with One-way ANOVA followed by Bonferroni's post hoc test. *p < 0.05; **p < 0.01; ***p < 0.001 compared with respective control.

Figure S4

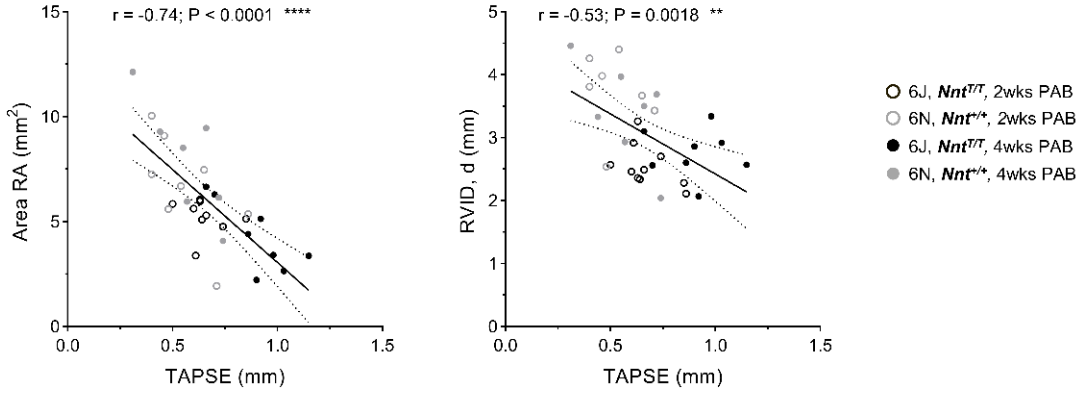

Figure S4. Linear correlations of tricuspid annular plane systolic excursion (TAPSE) with right atrial (RA) and right ventricular (RV) dilation. Negative linear correlations for 6J and 6N mice after 2 and 4 weeks of severe PAB are shown. N=32 mice. Statistical significance for Pearson correlation was tested.

Figure S5

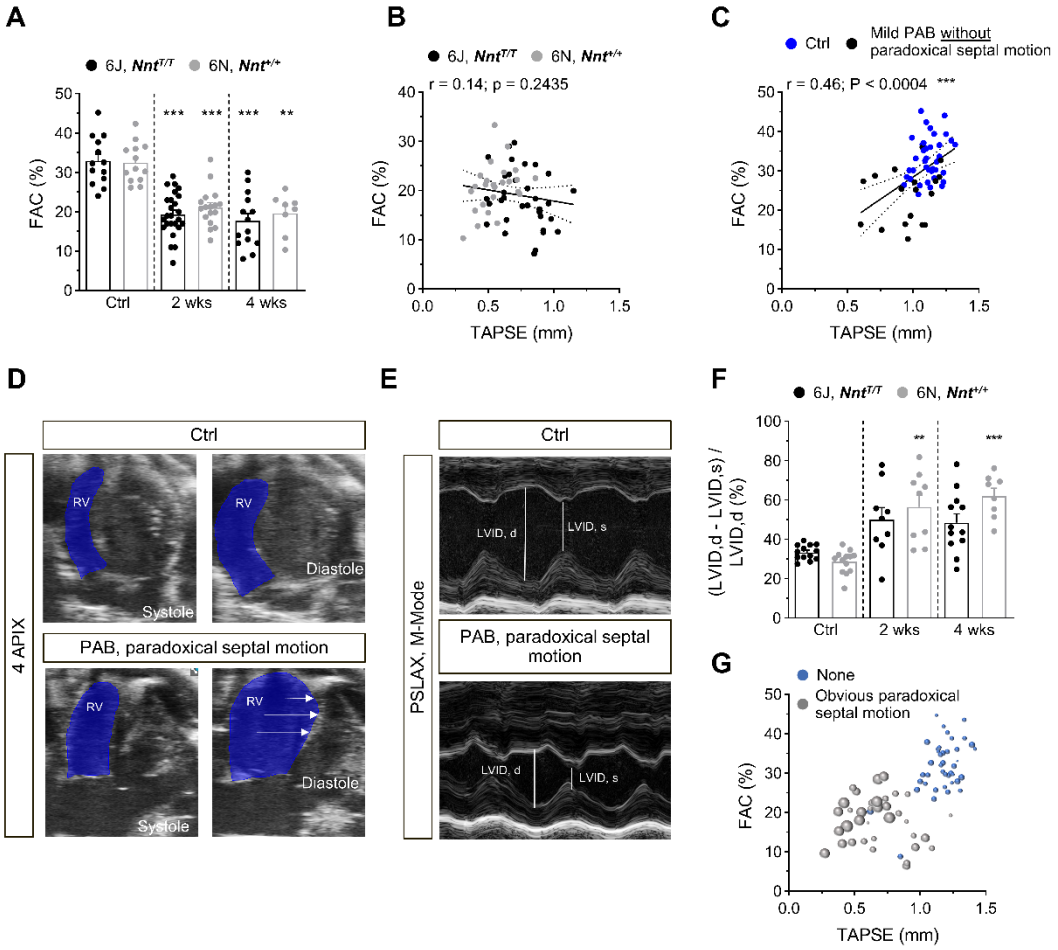

Figure S5. Paradoxical septal motion upon 4 weeks of severe pulmonary artery banding. A) Fractional area change (FAC) was significantly reduced in 6J and 6N mice after 2 and 4 weeks of pulmonary artery banding (PAB) (N=13/13/25/17/13/8 mice). B) FAC did not correlate with tricuspid annular plane systolic excursion (TAPSE) for 6J and 6N mice after 2 and 4 weeks of PAB (N=61 mice). C) FAC and TAPSE showed a significant correlation for 6J and 6N mice including PAB-exposed mice without paradoxical septal motion and untreated (Ctrl) mice (N=56 mice). D) Representative 2D apical 4-chamber view of an untreated (Ctrl) and PAB-treated mouse. Paradoxical septal motion resulted in an increase of diastolic right ventricular (RV) area, which falsely enlarges FAC values. E) Representative parasternal long axis view (PSLAX) in motion mode (M-Mode) indicating paradoxical septal motion upon PAB leading to decreased systolic (s) and diastolic (d) left ventricular internal diameter (LVID). F) The degree of paradoxical septum motion reflected by the following formula ((LVID,d – LVID,s) / LVID, d) was increased in 6J and 6N mice after 2 and 4 weeks of PAB (N=13/13/24/17/12/8 mice). G) Correlation of FAC and TAPSE for ctrl mice and mice after 2 and 4 weeks of PAB. The degree of paradoxical septal motion was visualized by bubble size on a linear continuous scale (N=87 mice). Animals with obvious paradoxical septal motion observed in echocardiography are marked in grey. For

A and F statistical significance was calculated with a marginal linear mixed effect model followed by Bonferroni's post hoc test and in B and C statistical significance for Pearson correlation was tested. **p < 0.01; ***p < 0.001 compared with respective control.

Figure S6

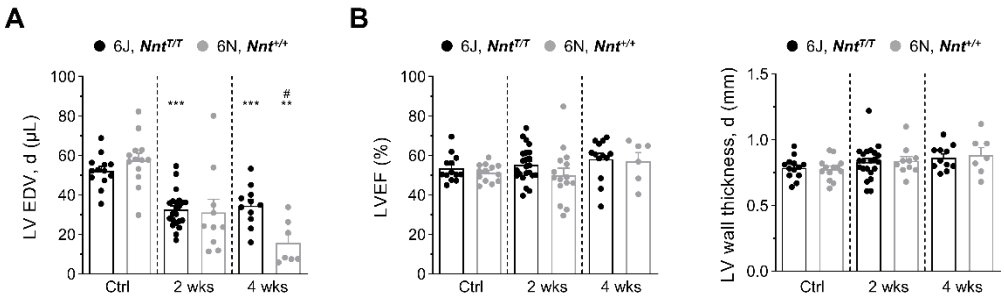

Figure S6. Left ventricular morphology and function of 6J and 6N mice upon 4 weeks of severe pulmonary artery banding. A) Left ventricular (LV) end-diastolic volume (EDV, d) was significantly diminished after 2 and 4 weeks of PAB. B) LV ejection fraction (EF) and wall thickness was not altered upon PAB (N=13/13/22/13/15/6 mice). Statistical significance was calculated with a marginal linear mixed effect model followed by Bonferroni's post hoc test. **p < 0.01; ***p < 0.001 compared with respective control; $^{\#}$p < 0.05 compared with corresponding 6J.

Figure S7

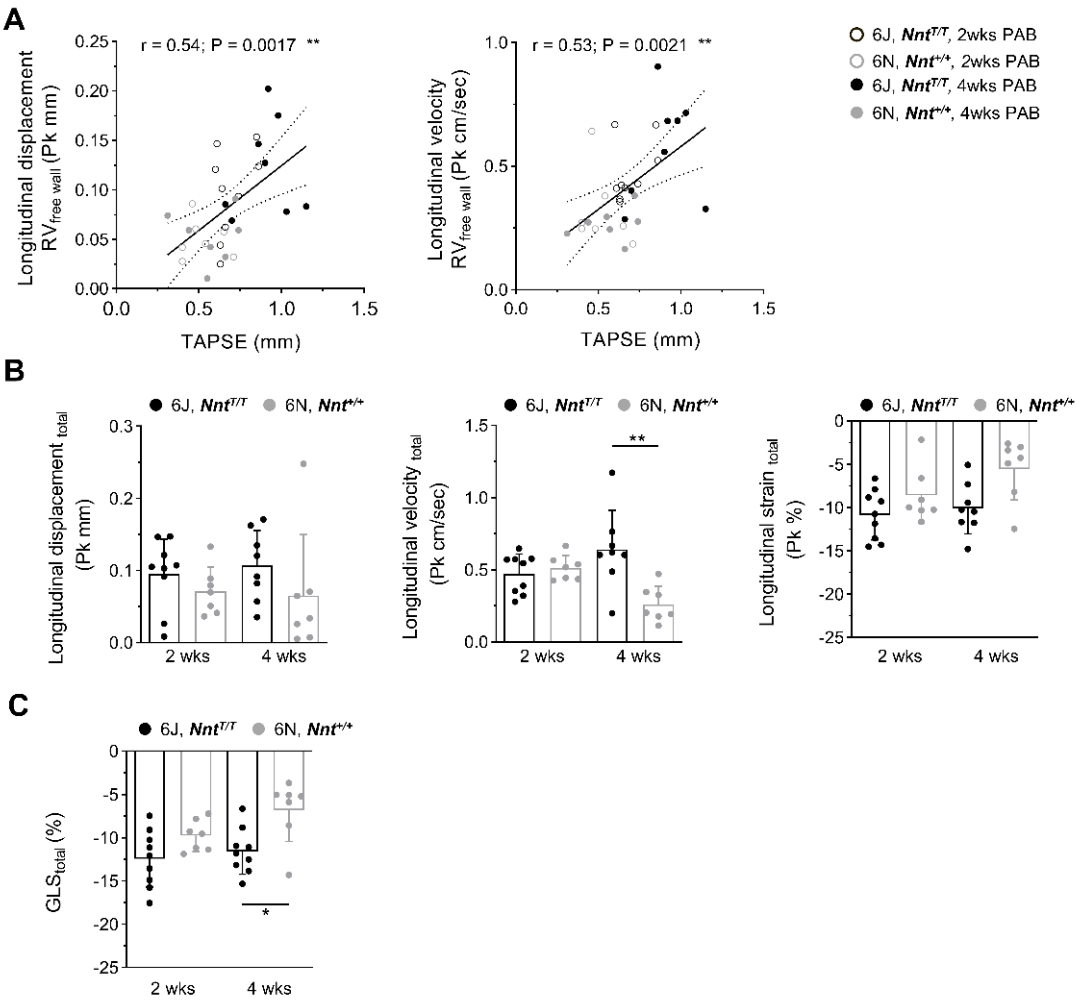

Figure S7. Longitudinal strain in 6J and 6N mice upon 4 weeks of severe PAB. A) Longitudinal displacement and velocity of the RV free wall of 6J and 6N mice after 2 and 4 weeks of PAB showed significant correlations with tricuspid annular plane systolic excursion (TAPSE) (N=31 mice). Statistical significance for Pearson correlation was tested. B) Longitudinal displacement, velocity, strain and, C) global longitudinal strain (GLS) of RV free wall and septum are shown, which demonstrates significantly impaired longitudinal velocity and GLS in 6N mice compared with 6J mice after 4 weeks of PAB (N= 7-9 mice). Statistical significance was calculated with One-way ANOVA followed by Bonferroni's post hoc test. *$p < 0.05$; **$p < 0.01$.

Figure S8

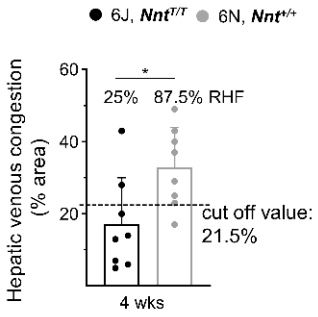

Figure S8. Hepatic venous congestion in 6J and 6N mice to identify right heart failure upon 4 weeks of severe pulmonary artery banding. The cut off value of 21.5% for the area of hepatic venous congestion as calculated by a receiver operating characteristics analysis identifies 25% of 6J and 87.5% of 6N mice to exhibit right heart failure (N=8/8 mice). Statistical significance was calculated with two-tailed unpaired Student's t-test. *p < 0.05.

Figure S9

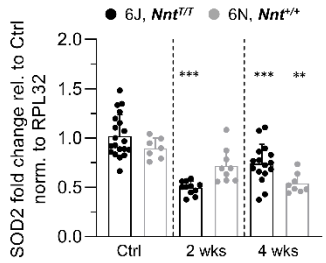

Figure S9. mRNA expression of SOD2 in 6J and 6N mice. mRNA expression of superoxide dismutase 2 (SOD2) was significantly lower in RV of 6J mice after 2 weeks of PAB and in 6J and 6N mice after 4 weeks of PAB (N=20/7/11/9/16/8 mice). Statistical significance was calculated with One-way ANOVA followed by Bonferroni's post hoc test. **p < 0.01; ***p < 0.001.

Figure S10

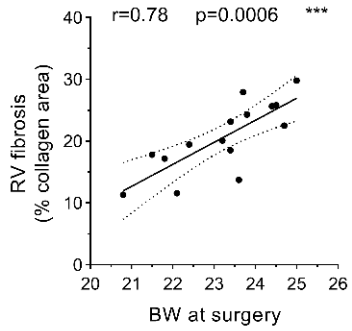

Figure S10. Correlation of mouse body weight at time of PAB surgery with the degree of right ventricular fibrosis. Baseline body weight of 6J and 6N mice showed a strong significant linear correlation with the fibrotic area as assessed from picrosirius red staining in RV sections 4 weeks after PAB. N=15 mice. Statistical significance for Pearson correlation was tested.

2. Supplemental Methods

Animal Experimental Protocols

For each PAB group, 14 mice were used. N-numbers below 14 are due to animals that died during surgery or thereafter. Data from echocardiography in Fig. 2 and Fig. 5 for PAB-exposed 6J and 6N mice after 1, 2 or 4 weeks include data from mice with final investigation after the later time points, respectively (longitudinal investigations). Baseline echocardiography was performed in all mice 1-3 days prior to PAB surgery and at indicated time points after surgery. For PAB, buprenorphine (0.1 mg/kg body weight (bw); Essex Pharma, Munich, Germany) was applied subcutaneously (s.c.) 30 min before. Mice were anaesthetized with inhalation of isoflurane (1.5-2 %, Baxter, Deerfield, IL, USA), ventilated and placed on a heating pad. After intercostal incision the pulmonary artery (PA) was identified and a titanium clip was placed between arterial root and bifurcation. The clip diameter was 450 µm (26 gauge (G)), 350 µm (28 G) or 300 µm (30 G) as indicated, respectively. The bw of mice was 24.4 ± 1.1 g (22.4 to 25.9 g) for 26 G, 25.2 ± 1.5 g (21.8 to 26.5 g) for 28 G and 22.2 ± 2.0 g (20.3 to 25.8 g) for 30 G PAB. The ideal bw was titrated in preliminary experiments based on PA velocity time integral 3 days after surgery. The thorax was closed and animals were allowed to recover. For analgesia, animals received s.c. buprenorphine 4 hours after surgery and once the next day (0.1 mg/kg bw). In addition, tramadol (1 mg/ml drinking water, Ratiopharm, Ulm, Germany) was given from one day before surgery until 3 days after via the drinking water. For final organ harvest, mice received s.c. analgesia with buprenorphine (0.1 mg/kg bw) 30 min before and were deeply anaesthetized with isoflurane (3%). Blood was drawn by apical puncture and the heart was excised and flushed with saline. Atria were removed and the right ventricle was separated from left ventricle and septum, weighed and processed for further analysis. Liver was excised and processed for histology.

Immunohistochemistry and Immunofluorescence

Formalin-fixed, paraffin-embedded RV were cut to sequential 5 µm cross-sections (30 sections in 5 sequential levels, distance between levels was 100 µm, respectively), deparaffinized and subjected to heat-induced antigen retrieval. For analysis of cardiomyocyte hypertrophy and capillary density, sections were incubated with Alexa Fluor 594-conjugated wheat-germ agglutinin (WGA, Thermo Fisher Scientific, Waltham, MA, USA) and Alexa Fluor conjugated-isolectin from *Griffonia simplicifolia* (GSI-B4, Thermo Fisher Scientific, Waltham, MA, USA). For analysis of 8-hydroxy-deoxyguanosine (8-OHdG), rabbit IgG to 8-OHdG (Thermo Fisher Scientific) was used diluted 1:500 followed by alkaline phosphatase conjugated secondary antibody (ImmPRESS-AP polymer, Vector Laboratories, Burlingame, CA, USA). Apoptotic nuclei were identified by terminal deoxynucleotidyl transferase-mediated dUTP Nick End labeling (TUNEL) method using In situ Cell Death detection kit (Merck, Darmstadt, Germany).

Images were acquired with a BZ9000 or BZ-X800 microscope (Keyence). At least 3 RV sections per level were analyzed in 40x magnification (resulting in at least 14 images per level). For 8-OHdG staining, level one and two were analyzed. A hue threshold was determined using staining with omitted first antibody (negative control) and area of positive immunoreactivity per total area of nuclei was quantified using ImageJ. For murine RV, cardiomyocyte nuclei with positive staining were counted manually in a blinded fashion, in addition. Cardiomyocyte cross sectional area from WGA staining and capillary count from GSI-B4 staining were analyzed in one level of RV tissue using a JavaCyte macro as described previously (1). TUNEL-positive nuclei were counted in a blinded fashion in level 1 and 2 for murine RV and numbers per high power field were calculated.

Quantitative Real Time PCR

Total mRNA was isolated from murine frozen tissues using the miRNeasy Micro Kit (Qiagen, Hilden, Germany) following the manufacturer´s standard protocol. Reverse transcription was performed for 30 min at 42 °C using dNTP Mix (10 mM each, VWR, Radnor, PA, USA) and SuperScript II Reverse Transcriptase (Thermo Fisher Scientific). qPCR was carried out on StepOnePlus (Applied Biosystems, Foster City, CA, USA) using Maxima Probe/ROX qPCR Master Mix (Thermo Fisher Scientific) for NPPA (sense: CAGAGACAGCAAACATCAGA, antisense: CAGGGTGATGGAGAAGGA), NPPB (sense: GGCTGTAACGCACTGAAG, antisense: CAGGCAGAGTCAGAAACTG), MYH6 (sense: CGCTTTGGGAAATTCATCAG, antisense: TCCAGAAGGTAGGTCTCTATG) and MYH7 (sense: TCTGCACAGAGAAAATCTGAAC, antisense: CCTGGAGACTTTGTCTCATTG). $2^{-\Delta CT}$ was calculated. For detecting mitochondrial copy number, quantitative real time PCR on DNA level was performed. Total DNA was isolated from murine frozen tissues using the Pure Link Genomic DNA Kit (Life Technologies, Carlsbad, CA, USA) following the manufacturer´s standard protocol. RT-PCR was carried out on StepOnePlus (Applied Biosystems, Foster City, CA, USA) using HotStarTaq DNA Polymerase (Qiagen, Hilden, Germany) according to the manufacturer's instructions. Three specific primer sequences targeting mitochondrial DNA (mtDNA) were as follows: mtDNA1 (sense: ATCCACTAAACACCCCACCC, antisense: GGATTGAGCGTAGAATGGCG); mtDNA2 (sense: ATCAGCACAATTTGGCCTCC, antisense: TGAAACTGGTGTAGGGCCTT); mtDNA3 (sense: GCACCTACCCTATCACTCACA, antisense: TGGGTGTGGTATTGGTAGGG). Primer pairs specifically binding to genomic DNA were used as reference: gDNA1 (sense: GCTCACACTGAATTCACCCC, antisense: CTCCCCAGTAGACGGTCTTG); gDNA2 (sense: ATGGATCTCCTGAAGGTGCTG, antisense: GTGCTGCCTTGAGACCGAA). $2^{-\Delta CT}$ was calculated and mtDNA copy number was shown as expression fold change normalized to the average of expression in 6J mice.

3. Supplemental References

1. Winters J, von Braunmuhl ME, Zeemering S, Gilbers M, Brink TT, Scaf B, et al. JavaCyte, a novel open-source tool for automated quantification of key hallmarks of cardiac structural remodeling. Sci Rep. 2020;10(1):20074.